# Comprehensive Examination of Mesophases Formed by DMPC and DHPC Mixtures

Thad A. Harroun,*,† Martin Koslowsky,† Mu-Ping Nieh,†,‡ Charles-François de Lannoy,† V. A. Raghunathan,§ and John Katsaras*,†

*Steacie Institute for Molecular Sciences, National Research Council, Chalk River, Ontario K0J 1J0, Canada, Department of Physics, University of Guelph, Guelph, Ontario N1G 2W1, Canada, and Raman Research Institute, Bangalore 560 080, India*

*Received January 4, 2005. In Final Form: March 7, 2005*

Mixtures of long- and short-chain phospholipids, specifically 14:0 and 6:0 phosphatidylcholines (DMPC and DHPC), have been used successfully in NMR studies as magnetically alignable substrates for membrane-associated proteins. However, recent publications have shown that the phase behavior of these mixtures is much more complex than originally thought. Using polarized light microscopy and small-angle neutron scattering, phase diagrams of DMPC/DHPC mixtures at molar ratios of 2, 3.2, and 5 have been determined. Generally, at temperatures below the main-chain melting transition of DMPC ($T_M = 23$ °C), an isotropic phase of disklike micelles is found. At high temperatures ($T > 50$ °C), a lamellar phase consisting of either multilamellar vesicles (MLV) or extended lamellae is formed, which at low lipid concentrations (e.g., MLV) coexists with an excess of water. At intermediate temperatures and lipid concentrations, a chiral nematic phase made up of wormlike micelles was observed.

## 1. Introduction

Mixtures of long-chain phospholipids and short-chain detergents have emerged as important substrates for NMR studies of biomolecules. These mixtures exhibit different liquid crystalline phases depending on total lipid concentration, mixing ratios of the constituents, and temperature. Of particular interest are phases that can be aligned in a magnetic field, either spontaneously or on doping with a lanthanide series ion. Such systems have been used to align both hydrophilic and hydrophobic macromolecules for high-resolution NMR studies.[1−4]

The canonical recipe of this class of amphiphilic systems is the mixture of the 14:0 and 6:0 hydrocarbon chain phosphatidylcholines, DMPC and DHPC, respectively.[5,6] The system is characterized by the molar ratio of long-to-short-chain lipids $Q$ = [DMPC]/[DHPC], and the total weight percent of lipid, $c_{lp}$. These mixtures are generally assumed to consist of disklike micelles, often called bicelles, with the long-chain lipid forming the flat region of the disk and the short-chain lipid forming the curved rim.[6] Although some authors have pointed out that this model does not adequately describe the physical properties of the system for $Q \geq 1$ and for temperatures at which magnetic alignment takes place,[7,8] the assumption of the lipid aggregates forming bilayered micelles persists in the literature.[9−12]

Until recently, the main proposed alternative to the bicelle morphology has been that of perforated lamellar sheets, essentially the inverse model to the bicelle.[13,14] Although this model is consistent with fluorescence and NMR data, it still does not explain the high viscosity of samples around room temperature. There has also been some speculation about the formation of interconnected lipid aggregates in these mixtures.[5] Moreover, there have only been a few incomplete papers dealing with the thermodynamic phase behavior of DMPC/DHPC mixtures.[8,13,15−18]

Recently, van Dam et al.[19] and Nieh et al.[20] have proposed a new paradigm for the phase behavior of DMPC/DHPC mixtures when $1 < Q < 5$. Using cryotransmission electron microscopy (TEM) and dynamic light scattering, van Dam presents evidence for a new lipid aggregate morphology, consisting of elongated, quasi-cylindrical micelles, in an intermediate range of temperatures and low lipid concentrations, that is, <5 wt %. The morphology and onset temperature of these micelles show both a strong $Q$ and temperature dependence. At higher and lower temperatures, van Dam observed multilamellar vesicles (MLV) and bicelles, respectively. Independently, using polarized optical microscopy (POM) and small-angle

* Corresponding authors.
† National Research Council.
‡ University of Guelph.
§ Raman Research Institute.

(1) Whiles, J. A.; Deems, R.; Vold, R. R.; Dennis, E. A. *Bioorg. Chem.* **2002**, *30*, 431−442.
(2) Andersson, A.; Almqvist, J.; Hagn, F.; Mäler, L. *Biochim. Biophys. Acta* **2004**, *1661*, 18−25.
(3) Lancelot, N.; Elbayed, K.; Biancob, A.; Piottoa, M. *J. Biomol. NMR* **2004**, *29*, 259−269.
(4) Sizun, C.; Aussenac, F.; Grelard, A.; Dufourc, E. J. *Magn. Reson. Chem.* **2004**, *42*, 180−186.
(5) Sanders, C. R., II; Schwonek, J. P. *Biochemistry* **1992**, *31*, 8898−8905.
(6) Vold, R. R.; Prosser, R. S. *J. Magn. Reson. B* **1996**, *113*, 267−271.
(7) Sanders, C. R.; Prosser, R. S. *Structure* **1998**, *6*, 1227−1234.
(8) Nieh, M.-P.; Glinka, C. J.; Krueger, S.; Prosser, R. S.; Katsaras, J. *Biophys. J.* **2002**, *82*, 2487−2498.
(9) Zandomeneghi, G.; Tomaselli, M.; Williamson, P. T. F.; Meier, B. H. *J. Biomol. NMR* **2003**, *25*, 113−123.
(10) Minto, R. E.; Adhikari, P. R.; Lorigan, G. A. *Chem. Phys. Lipids* **2004**, *132*, 55−56.
(11) Inbaraj, J. J.; Nusair, N. A.; Lorigan, G. A. *J. Magn. Reson.* **2004**, *171*, 71−79.
(12) Li, X.; Goodson, B. M. *Langmuir* **2004**, *20*, 8437−8441.
(13) Gaemers, S.; Bax, A. *J. Am. Chem. Soc.* **2001**, *123*, 12343−12352.
(14) Rowe, B. A.; Neal, S. L. *Langmuir* **2003**, *19*, 2039−2048.
(15) Raffard, G.; Steinbruckner, S.; Arnold, A.; Davis, J. H.; Dufourc, E. J. *Langmuir* **2000**, *16*, 7655−7662.
(16) Luchette, P. A.; Vetman, T. N.; Prosser, R. S.; Hancock, R. E. W.; Nieh, M.-P.; Glinka, C. J.; Krueger, S.; Katsaras, J. *Biochim. Biophys. Acta* **2001**, *1513*, 83−94.
(17) Nieh, M.-P.; Glinka, C. J.; Krueger, S. *Langmuir* **2001**, *17*, 2629−2638.
(18) Sternin, E.; Nizza, D.; Gawrisch, K. *Langmuir* **2001**, *17*, 2610−2616.
(19) van Dam, L.; Karlsson, G.; Edwards, K. *Biochim. Biophys. Acta* **2004**, *1664*, 241−256.
(20) Nieh, M.-P.; Raghunathan, V. A.; Glinka, C. J.; Harroun, T. A.; Pabst, G.; Katsaras, J. *Langmuir* **2004**, *20*, 7893−7897.

10.1021/la050018t CCC: $30.25 
Published on Web 05/12/2005

neutron scattering (SANS), we have reached similar conclusions for $2 \leq Q \leq 5$. Samples with a total lipid concentration ($c_{lp}$) of 25 wt % are found to exhibit a chiral nematic phase made up of linear aggregates (e.g., wormlike micelles) at intermediate temperatures. These studies also reveal an isotropic phase made up of bicelles at low temperatures and a lamellar phase consisting of perforated bilayers at higher temperatures.[20,21]

These recent data by Nieh et al. point to a model of orientationally ordered wormlike micelles for the magnetically alignable phase. It is thought that this discovery may have important implications for developing uses of bicellar mixtures, such as for protein crystallization,[22] or for capillary electrophoresis of amphiphilic peptides and drug molecules.[23,24]

Because previous phase diagrams did not identify the wormlike micellar phase and recent reports[6,15] are incomplete with respect to concentration and temperature, there is a need for a more detailed phase diagram with respect to this widely studied and used system. Therefore, in this paper, we present comprehensive phase diagrams of DMPC and DHPC mixtures, for $Q = 2$, 3.2, and 5, as determined by POM and SANS.

Compared to van Dam, much wider ranges of lipid concentrations and temperatures are examined. The phase behavior of the $Q = 3.2$ and 5 samples are similar. An isotropic phase (I), consisting of bicelles, is found in both systems at low temperatures and lipid concentrations between 1 and 40 wt %. On heating, the isotropic phase transforms into a chiral nematic phase (N*), made up of long wormlike micelles. The I → N* transition nearly coincides with the chain-melting transition of DMPC over an expanded range of $c_{lp}$, beyond which it quickly decreases with increasing $c_{lp}$. At higher temperatures a lamellar phase consisting of MLV or extended lamellae is obtained, which coexists with excess water at lower lipid concentrations. The behavior at $Q = 2$ is somewhat different, with the isotropic phase being stable over a much larger temperature range. Furthermore, this system also shows the coexistence of two isotropic phases at low $c_{lp}$, one of which is much more viscous than the other.

It should be pointed out that the term "bicellar mixture" is commonly used in the literature to refer to DMPC/DHPC mixtures, whereas "bicelles" are just one of the morphologies formed by these lipid mixtures.

## 2. Materials and Methods

1,2-Dimyristoyl-*sn*-glycerol-3-phosphatidylcholine (DMPC) and 1,2-dihexanoyl-*sn*-glycero-3-phosphatidylcholine (DHPC) were purchased, as lyophilized powders, from Avanti Polar Lipids (Alabaster, AL) and used as received. Samples were prepared from stock chloroform solutions in molar ratios, $Q$, of $2.00 \pm 0.04$, $3.20 \pm 0.06$, and $5.0 \pm 0.1$. Predetermined amounts of this solution to make ~0.5 mL final volume samples were dispensed, and the chloroform was evaporated under a dry stream of helium. Samples were then left in a vacuum for >3 h to remove any traces of the solvent. Ultrapure $H_2O$ (resistivity of 18.3 MΩ-cm) was added to make solutions of 2−50 wt % lipid, in 2−5 wt % steps. Pure $D_2O$ was used to make the $Q = 2$ samples. The reported weight percent values for these samples are based on the mass of $D_2O$. No buffer or salt was added to the solution. Samples were then subjected to a series of vortex and heating and cooling cycles over the next several days to ensure thorough mixing. Samples were stored at 1 °C, which is generally the isotropic phase of bicelles.

For POM, samples were loaded by capillary action into flattened capillaries (VitroCom Inc., Mountain Lakes, NJ) (inside dimensions of 0.1 × 2 mm, 0.1 mm wall thickness), and the ends were flame-sealed. Some room temperature, high-viscosity samples were cooled to the less viscous isotropic phase and then taken up in the capillaries. Temperature was controlled by a Linkam THMS600 microscope stage (Surrey, U.K.) to ±0.1 °C. Samples were observed under 10× magnification objective, whereas the spatial dimensions of digital micrographs were calibrated using a micrometer.

Separate SANS $Q = 3.2$ and 5 samples were mixed from lyophilized powder, although in $D_2O$ instead of $H_2O$ for better scattering contrast. SANS data were taken on the 30 m SANS beamline at NIST (Gaithersburg, MD). Detailed descriptions of data collection and analysis are given elsewhere.[25] On the other hand, neutron diffraction in the high $q$ regime ($q = 4\pi \sin\theta/\lambda$, where $2\theta$ is the scattering angle and $\lambda$ the neutron wavelength) requires less sample, and as such the same $Q = 2$ samples were shared between diffraction and POM. Diffraction data were collected on the N5 and E3 spectrometers (Chalk River, ON) using 2.37 Å neutrons.

## 3. Results

Determination of phase transition temperatures primarily relies upon abrupt changes in POM textures when the temperature is changed. In certain cases, the phase transition is well-defined, within 1 °C, and, most importantly, reversible. Such transitions typically involve the appearance of the isotropic phase, or the disappearance of MLV. In cases when the changes in texture are more gradual, or a coexistence of phases is seen, samples were allowed to equilibrate from 1 to 12 h at the set temperature. The phase boundaries were refined by approaching them from both above and below the transition temperature. It is important to note that the phase boundaries are determined from the observed reversibility of the phase changes, which is a strong indicator of the thermodynamic stability of the phases. Thus, equilibration for more than a few hours may change the boundaries around the coexisting regions slightly, but not the morphology of a particular phase.

When POM data were difficult to interpret, such as at high $c_{lp}$, the phases were identified with the aid of SANS data. However, even at other $c_{lp}$, SANS data were used to confirm the phases identified from POM textures. Nieh and co-workers have previously reported on the size of bicelles[8] and MLV[25] from SANS data and, most recently, the characteristic SANS signature of wormlike micelles.[20]

The phase diagrams for $Q = 3.2$, 5, and 2 are shown in Figures 1−3, respectively. Two regions of interest, namely, $Q = 2$ samples at low $c_{lp}$ and $Q = 5$ samples at high $c_{lp}$, for which the combined SANS and POM data were inadequate or ambiguous for precise phase characterization, will be discussed in the following sections.

**3.1. Phases at $Q = 3.2$.** We begin with the $Q = 3.2$ ratio of DMPC/DHPC, because in the literature it is cited as lying in the regime of the best alignable samples in the presence of an applied magnetic field.[26] Figure 1 shows the phase diagram determined for $Q = 3.2$. An isotropic phase with no birefringence occupies a region below $T =$ 20 °C and $c_{lp}$ between 5 and 35 wt %. Samples in this region are visibly clear and have a viscosity comparable to that of water. No birefringence is seen even at the highest concentrations, indicating that most likely bicelles do not form a nematic phase. SANS data of this phase show a flat $I(q)$ at low $q$, which can only be fitted with a

(21) Nieh, M.-P.; Raghunathan, V. A.; Glinka, C. J.; Harroun, T. A.; Katsaras, J. *Macromol. Symp.* **2005**, in press.
(22) Caffrey, M. J. *Struct. Biol.* **2003**, *142*, 108−132.
(23) Mills, J. O.; Holland, L. A. *Electrophoresis* **2004**, *25*, 1237−1242.
(24) Holland, L. A.; Leigh, A. M. *Electrophoresis* **2003**, *24*, 2935−2939.
(25) Nieh, M.-P.; Harroun, T. A.; Raghunathan, V. A.; Glinka, C. J.; Katsaras, J. *Biophys. J.* **2004**, *86*, 2615−2629.
(26) Struppe, J.; Whiles, J. A.; Vold, R. R. *Biophys. J.* **2000**, *78*, 281−289.

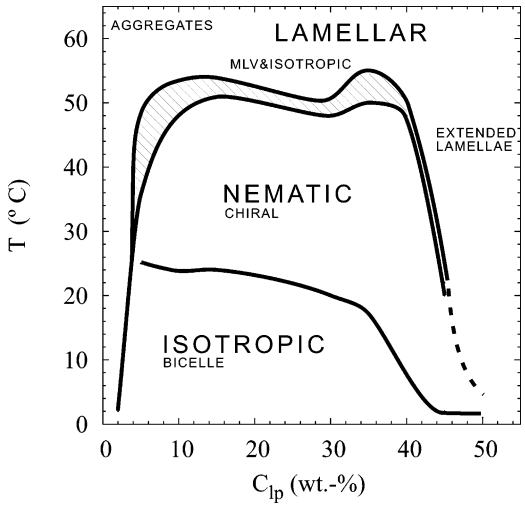


**Figure 1.** Phase diagram for $Q = 3.2$ DMPC/DHPC "bicellar" mixtures. The dominant phases as determined by POM are shown. The morphologies that make up these phases are indicated. The dashed line indicates some ambiguity in determining the exact phase transition, whereas the hatched area depicts the coexistence region of nematic and lamellar phases.

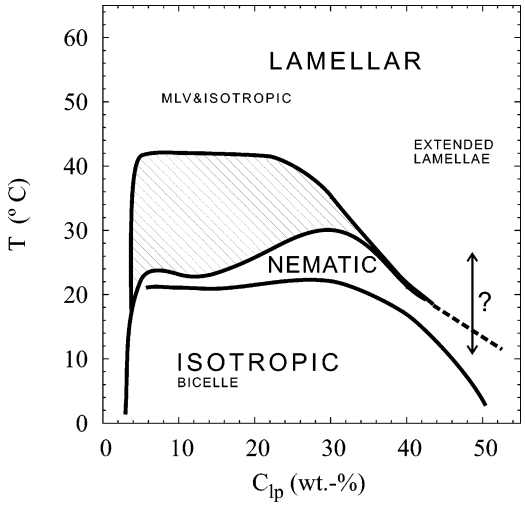


**Figure 2.** Phase diagram for $Q = 5.0$ DMPC/DHPC mixtures. The question mark indicates the region where the POM and SANS data were too ambiguous to conclusively determine the transition temperature and the morphology. The hatched area indicates a region of coexistence.

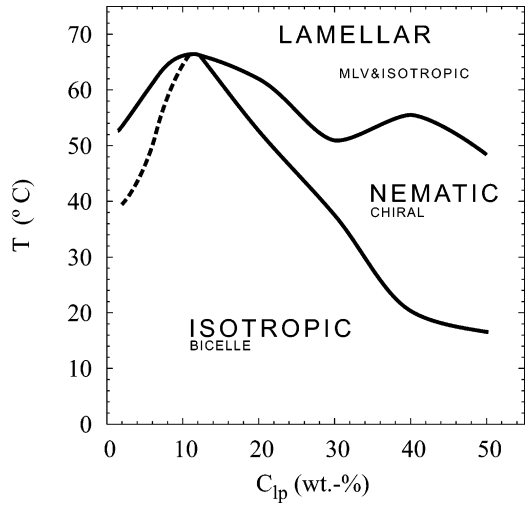


**Figure 3.** Phase diagram for $Q = 2.0$ DMPC/DHPC mixtures. The dashed line indicates the transition of the bicellar isotropic phase into two distinct isotropic phases (morphologies presently unknown), one of which is more viscous than the other.

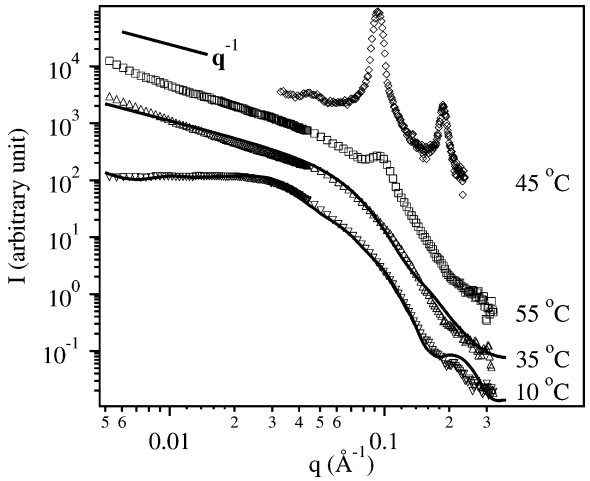


**Figure 4.** Examples of SANS data obtained from the various morphologies. The open symbols denote $Q = 3.2$ and $c_{lp} = 10$ wt % at temperatures of 10 (▽), 35 (△), and 55 (○) °C. These correspond to bicelles, nematic phase of elongated objects, and a MLV lamellar phase, respectively. (◇) $Q = 5$ and $c_{lp} = 45$ wt %, showing quasi-Bragg scattering from a smectic lamellar phase. Best fits to the bicelle and nemtic data are shown as a solid line.

model of a disk-shaped object. The measured thickness of the disks ranges from 45 to 55 Å, with a radius of 100−250 Å, which varies as a function of concentration. A best fit of the 10 wt % data is shown in Figure 4, using a disk-shaped model and a structure factor determined from a simulation of same-sized prolate hard Gaussian objects.[27]

In the intermediate temperature range a chiral nematic phase is found and was identified from the characteristic fingerprint texture.[25] The nematic phase, in general, consists of rodlike or disklike aggregates and has long-range orientational order but only a short-range positional order. When the constituent molecules are chiral, the preferred direction of orientation undergoes a spontaneous twist resulting in the characteristic fingerprint pattern seen under the microscope.[28] An example of the nematic phase for $Q = 3.2$ is given in Figure 5B. In practically all of the conditions examined the N* texture is colorless. In some high lipid concentration cases, such as those in Figure 5B, the texture remains the same as for other N* samples, but can appear colored.

In the absence of long-range positional order, the SANS pattern of the N* phase does not contain any sharp peaks, and only a broad peak corresponding to the average interparticle separation, as in a liquid, is observed. In the present system at small $q$, $I(q) \sim q^{-1}$, indicating the presence of elongated structures, possibly wormlike micelles. The typical SANS pattern can be seen in Figure 4 for a $Q = 3.2$ sample at 35 °C. The best fit is also presented in Figure 4, which incorporates a hybrid core−shell cylinder form factor and hard disk structure factor.[20] Typical radii used were between 25 and 30 Å. The length of the micelles is >2000 Å and is beyond our small $q$ limit. As a result, we cannot precisely determine the length of the wormlike micelles.

The nematic phase exists across a comparably wide range of temperatures for $Q = 3.2$. Samples in this phase

(27) Berne, B. J.; Pechukas, P. J. *Chem. Phys.* **1972**, *56*, 4213−4216.
(28) de Gennes, P. G.; Prost, J. *The Physics of Liquid Crystals*; Oxford University Press: Oxford, U.K., 1993.

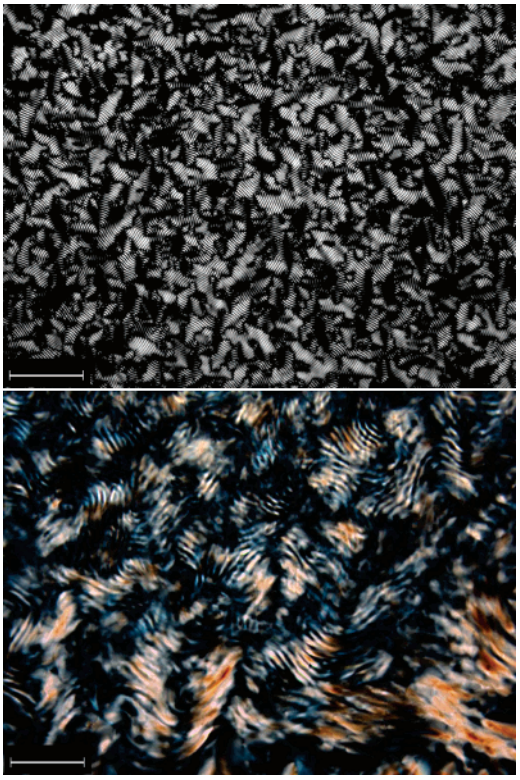

**Figure 5.** Examples of POM micrographs of nematic phases: (top) $Q = 2.0$, $c_{lp} = 20$ wt %, $T = 60.0$ °C; (bottom) $Q = 3.2$, $c_{lp} = 40$ wt %, $T = 22.6$ °C. The scale bar is 0.1 mm.

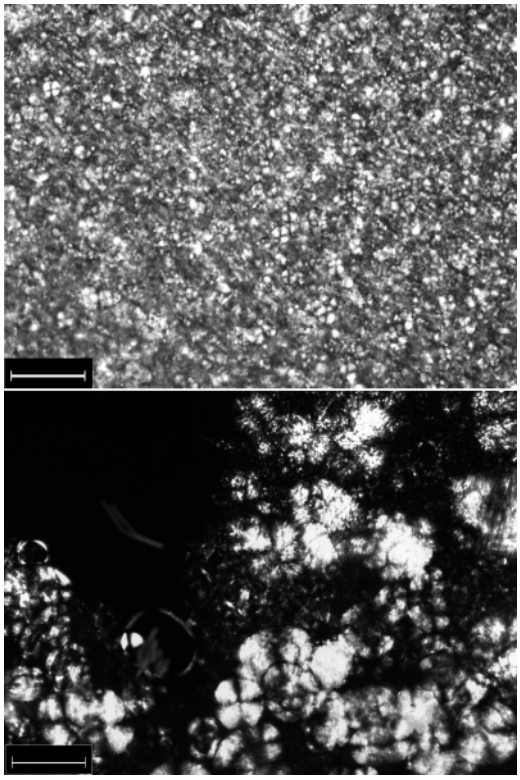

**Figure 6.** Examples of POM micrographs of the MLV phase: (top) $Q = 3.2$, $c_{lp} = 30$ wt %, $T = 50.0$ °C; (bottom) $Q = 5.0$, $c_{lp} = 5$ wt %, $T = 45.0$ °C. The scale bar is 0.1 mm.

are highly viscous, with the maximum viscosity being observed in the middle of the temperature range, which is consistent with unexplained observations reported previously.[29] The POM texture appears to be qualitatively similar across the range. The fingerprint texture takes at least 1 h to fully develop after the N* phase forms either from the isotropic or lamellar phases. The pitch of the helical structure, as determined from the periodicity of the fingerprint texture, ranges typically from 2 to 8 $\mu$m and does not seem to depend significantly on either temperature or concentration.

The nematic phase gives way to extended lamellae at temperatures >45 °C, with a narrow coexistence region <5 °C wide. Coexistence was determined by the appearance of separate domains of the fingerprint and lamellar textures. To confirm this coexistence, samples in this temperature range were typically incubated overnight. The lamellar phase contains a variety of high-density, extremely birefringent, and colorful defects (Figure 7A) and can be identified from the typical focal conic and "oily streak" textures. Oily streaks are disclination lines running through a highly aligned (planar) area of the sample, whereas focal conic defects give rise to so-called "fan" textures.[28] SANS data for smectic phases are all very similar, exhibiting multiple Bragg peaks at values of $q = 2\pi h/d$, where $h$ is an integer and $d \sim 60$ Å is the lamellar periodicity.

In dilute samples (e.g., < ~40 wt %) the lamellar phase is made up of MLV and coexists with an isotropic phase. Upon reaching the lamellar phase, MLV initially appear as a cloudlike POM texture, followed by the formation of spherical, highly birefringent objects with a "Maltese-cross" texture. Examples of MLV can be seen in Figure 6 and are persistent over a wide range of $c_{lp}$. At low lipid concentrations, 5 wt % and below, small spherical aggregates of lipid in an isotropic solution are observed. The formation of the lamellar phase was confirmed by SANS data, which show a quasi-Bragg peak corresponding to a lamellar periodicity, $d \sim 60$ Å. In Figure 4, the peak

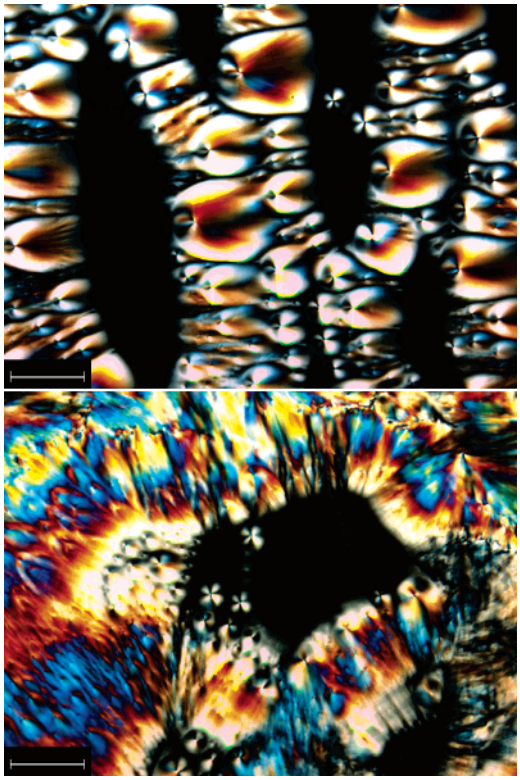

**Figure 7.** Examples of POM micrographs of smectic lamellar phases: (top) $Q = 3.2$, $c_{lp} = 45$ wt %, $T = 60.0$ °C; (bottom) $Q = 3.2$, $c_{lp} = 50$ wt %, $T = 30.0$ °C. The scale bar is 0.1 mm.

(29) Hwang, J. S.; Oweimreen, G. A. *Arab J. Sci. Eng.* **2003**, *28*, 43–49.

appears along with the characteristic $q^{-1}$ dependence of the nematic phase. This is consistent with the MLV/nematic coexistence seen by POM at this temperature.

**3.2. Phases at $Q = 5$.** The phase behavior of DMPC/DHPC mixtures at $Q = 5$ (Figure 2) is very similar to that at $Q = 3.2$, with the isotropic phases occupying much of the same region. For $Q = 5$, the most prominent change is the reduction of the pure nematic region. There was little difference in the textures exhibited by the chiral nematic phases of $Q = 3.2$ and $Q = 5$ samples. Instead, the range of coexistence between the MLV and chiral nematic phases is greatly increased for concentrations below 30 wt %. The exact onset of the nematic phase from the lamellar phase was difficult to determine. In the broad coexistence range, the nematic phase was often poorly formed for $Q = 5$ samples. In some cases it was possible to see a "flickering" effect near the interfaces between nematic and lamellar domains, resulting from the thermal fluctuations of the nematic director. At low $c_{lp}$, MLV aggregates were observed in an isotropic phase (probably made up of DHPC monomers) for all temperatures and concentrations below 2 wt %.

At high lipid concentrations, >40 wt %, POM data indicated several reproducible phase transitions between 5 and 30 °C; however, the resulting phases could not be identified. This is indicated by the dashed line and question mark in Figure 2. Neutron diffraction data show highly aligned lamellar Bragg peaks across this temperature range (data not shown), but changes in the lamellar spacing do not correspond to the transitions seen by POM. Instead, additional peaks appear in the small $q$ region, which may indicate a higher organization of defects in perforated bilayers. These peaks are very weak and are presently the topic of further investigation. At very low temperatures, these samples become isotropic.

**3.3. Phases at $Q = 2$.** For the final [DMPC]/[DHPC] molar ratio studied, we again find a chiral nematic phase sandwiched between lamellar and isotropic phases. For this molar ratio the isotropic phase occupies a much larger area in the phase diagram. The I → N* transition temperature increases with decreasing $c_{lp}$ below 30 wt %, up to a maximum of 66 °C at 12 wt %. This is well above the chain-melting transition temperature, $T_M = 23$ °C, of DMPC which nearly coincides with the I → N* transition for $Q = 3.2$ and 5.

At $c_{lp}$ below 12 wt % there is a region where two isotropic phases coexist. These two coexisting isotropic phases appear under the microscope as a dispersion of droplets with sharp boundaries. The onset of these dual isotropic phases is indicated by the dashed line in Figure 3. Moreover, it is noted that one of these phases is much more viscous than the other. To elucidate these morphologies, further SANS studies are required.

The chiral nematic fingerprint texture was found to be more pronounced for $Q = 2$ samples. The domains were significantly larger, and the orientation of the helical axis director was more uniform. This is evident in the micrograph shown in Figure 5. No noticeable coexistence between the lamellar and nematic phases is observed, with the transition being sharp and taking place within 2 °C. The lamellar phase is formed from MLV coexisting with an isotropic solution up to the highest $c_{lp}$ studied. This lamellar phase lacked the color and focal conic defects of the smectics found in higher $Q$ samples.

## 4. Discussion

The principal use of bicellar mixtures has been as magnetically alignable substrates for biomolecular NMR. However, bicellar mixtures are finding increasing uses without a magnetic field, such as protein crystallization[30] and electrokinetic chromatography.[23,24] In any case, it is important to have detailed structural information of the alignable phase of interest in order that the protein's environment is well characterized. The gross morphology of DMPC/DHPC mixtures at one concentration and in the absence of a magnetic field was recently reported by Nieh et al.[20] However, further work is needed to obtain detailed structural information across a wider range of concentrations and values of $Q$.

POM is a useful technique in the study of liquid crystalline materials, but has been used remarkably little in phospholipid studies.[31−33] Using POM, we have been able, for the first time, to accurately measure the phase boundaries across an extended range of lipid concentrations and temperatures, something not practically achievable by SANS alone.

The phases presented here differ from those determined by $^{31}$P NMR.[15] Although the region of lamellar and isotropic phases is in broad agreement with Raffard et al.,[15] they claimed the magnetically alignable phase to be made up of bicelles rather than wormlike micelles as determined by us. In addition, the morphology of entangled ribbons[20] is consistent with the high viscosity observed in the chiral nematic region of the phase diagram.[34] It should be pointed out that, although changes in the viscosity and turbidity are clear indicators of changes in the aggregate morphology, they do not give any direct structural information about the phases formed by the lipid aggregates. This is further complicated by the fact that a dramatic increase in viscosity can occur within the same phase on changing the temperature, as found here in the isotropic phase of the $Q = 2$ sample.

van Dam et al. identify four distinct morphologies for $Q \geq 1$ and low lipid concentrations (≤5 wt %): small disklike aggregates, cylindrical micelles, bilayers, and a coexistence of a micellar network with perforated bilayers. (Note that our definition of $c_{lp}$ is total weight percent, whereas for van Dam et al., it is the lipid to solvent mass ratio.) These phases correspond to our POM observations, even at higher concentrations, of isotropic (i.e., bicelles), chiral nematic (i.e., wormlike micelles), lamellar (i.e., MLV or extended lamellae), and chiral nematic/lamellar coexistence, respectively. It is important to note that at low concentrations, it is difficult to determine the exact bicelle to wormlike micelle transition temperature, because the chiral nematic phase may be preceded by an isotropic phase of wormlike micelles, which cannot be distinguished from a solution of bicelles by POM.

From the data presented above, it is clear that the thermodynamics and kinetics of phase formation are governed by the detergent-like behavior of DHPC. The comparison of short-chain lipid behavior to that of other amphiphillic detergents has previously been made.[35] Understanding lipid−detergent mixtures is of basic importance for the solubilization and reconstitution of membranes.[36] One important use for lipid−detergent mixtures is the formation of unilamellar lipid vesicles from lipids that would normally form a lamellar phase. These types of systems share a common mechanism for vesicle formation, where at high detergent concentrations the

(30) Faham, S.; Bowie, J. U. *J. Mol. Biol*. **2002**, *316*, 1−6.
(31) Powers, L.; Pershan, P. S. *Biophys. J.* **1977**, *20*, 137−152.
(32) Asher, S. A.; Pershan, P. S. *Biophys. J.* **1979**, *27*, 393−421.
(33) Huang, H. W.; Olah, G. A. *Biophys. J.* **1987**, *51*, 989−992.
(34) Struppe, J.; Vold, R. R. *J. Magn. Reson*. **1998**, *135*, 541−546.
(35) Hauser, H. *Biochim. Biophys. Acta* **2000**, *1508*, 164−181.
(36) For a review of lipid−detergent mixtures, see the issue of *Biochim. Biophys. Acta: Biomembranes* **2000**, 1508.

amphiphiles typically self-aggregate into small micellar clusters. The micelle to vesicle transition is driven by depleting the detergent from solution by methods such as dilution, dialysis, and chemical reaction. Between micelles and vesicles there may exist transitional intermediate phases, such as ribbon-like micelles reported here and in the literature.[37]

It is reasonable to expect the aggregate size to depend on the amount of DHPC incorporated by it. We speculate that at low DHPC content, perforated bilayers are formed with DHPC lining the rim of the hole. With increasing DHPC concentration, the density of curvature defects in the bilayer increases, ultimately breaking up into ribbon-like aggregates. These in turn are transformed into disklike bicelles at higher DHPC concentrations. From our data, as well as those of van Dam et al., it appears that these morphological changes are not gradual, but abrupt, involving a narrow range over which two morphologies coexist. The bicelle to wormlike micelle transition seems to be related to the transition temperature of DMPC for $Q = 3.2$ and 5 samples (Figures 1 and 2). This $Q$ independence may also apply to the $Q = 2$ samples because, as stated previously, an isotropic phase of wormlike micelles cannot be distinguished by POM from a solution of bicelles. The association of the bicelle to nematic transition coinciding with the main transition temperature of DMPC may be the result of immiscibility between gel phase DMPC and liquid crystalline DHPC. Furthermore, the nematic to lamellar transition may possibly be attributed to a loss of DHPC from the elongated micelles to solution, resulting in MLV from the coalescence of the elongated micelles. This may explain the $Q$ dependence of the nematic to lamellar phase transition observed in all of the samples (Figures 1−3).

It is interesting to note that the DHPC content of the aggregates, and hence their morphology, can be controlled not only by choosing the sample composition directly but also by altering the temperature. DHPC released from mixed-lipid aggregates may disperse in the aqueous solution in the form of monomers or micelles. The reported critical micellar concentration (cmc) for DHPC is rather high, in the range between 5.2 and 7.2 mg/mL (11−15 mM);[35] however, we are not aware of a DHPC cmc measurement as a function of temperature. In comparison, the total DHPC content of a 20 wt %, $Q = 5$, sample is ∼75 mM, implying that a significant part of this lipid can be accommodated as monomers in the aqueous solution. However, a direct measurement of DHPC concentration in solution as a function of temperature is required to verify this.

Electrostatics do not play an important role in this study. No salt or buffer was added to solution, and any ions present are from the stock lipid. Thus, for the purposes of this study we assume that there is very little, if any, ionic strength in solution or surface potential on the bilayer. The "hydration force" arising from the dipole potential is assumed to decay exponentially with a length of 1−2 Å.[38]

It is important to note that the present experiments have been carried out in the absence of a magnetic field. Therefore, the question remains of whether the chiral nematic phase undergoes a transition to another phase in a magnetic field. To our knowledge, there has only been one structural measurement performed in both the presence and absence of the magnetic field. Katsaras et al. state that the morphologies formed by bicellar mixture lipids are independent of the presence of a magnetic field.[39]

van Dam et al. assert that the magnetically alignable phase is not wormlike micelles, but rather perforated lamellae, which they observed to form at elevated temperatures from the fusion of wormlike micelles. They further point out that NMR data are consistent with such a phase: Two peaks in the $^{31}$P spectrum, with relative intensities roughly equal to $Q$, are assignable to DMPC and DHPC[5,15,40] In addition, the absence of $^{1}$H NOESY DMPC/DHPC cross-peaks[18] also suggests that the lipids are separated into different domains. However, we dispute their statement that the onset of turbidity and the concomitant drop in viscosity, which is now understood to correspond to the onset of lamellar phases, is the indicator of magnetic alignment. It is the *increase in viscosity with temperature* which corresponds very nearly with magnetic alignment[15,34] and also corresponds to the chiral nematic phase presented here. If in the "bicelle" $^{31}$P spectrum the DMPC/DHPC peak separation is an indication of the onset of an aligned phase and the upfield shift of the spectrum indicates greater alignment,[15,41] then the reported temperatures of a highly aligned stable morphology occur only across the range of the presently identified chiral nematic phase. It is from this observation of increased viscosity and magnetic alignment as a function of temperature, which happen to coincide with the temperature range of the chiral nematic shown in Figures 1−3, that we reach the conclusion that the magnetically alignable phase is made up of wormlike micelles and not perforated lamellae.

We speculate that the cross section of wormlike micelles is most probably that of a DMPC bilayer with edges coated by a DHPC monolayer. In this sense, the cross section is similar in profile to a bicelle, which may help to explain why NMR data have been interpreted in terms of a bicelle model. However, TEM data seem to indicate the micelles to be nearly cylindrical. The diameters of the micelles seen by TEM and SANS are well below the ∼100 Å radius of the typical bicelle for $Q > 2.0$, strongly indicating that micelles are unlikely to form a columnar phase of stacked bicelles.

## 5. Concluding Remarks

In conclusion, using POM and SANS data we have constructed comprehensive phase diagrams of DMPC/DHPC mixtures at molar ratios, $Q$, of 2, 3.2, and 5. For all $Q$ values three mesophases are observed. Over a wide range of lipid concentrations at low temperatures, an isotropic phase, identified by SANS as consisting of bicelles, is found. At high temperatures, we find either a pure lamellar phase (e.g., extended lamellae) or a MLV− isotropic coexistence. At intermediate temperatures, a chiral nematic made up of elongated aggregates is observed, most probably wormlike micelles.[19−21] Presently, there are some regions of ambiguity, especially for high lipid concentration $Q = 5$ mixtures and for very low lipid concentration $Q = 2$ mixtures, which will be a topic of future investigations.

**Acknowledgment.** We thank J. Pencer for many useful discussions and the Advanced Foods and Materials Network (Networks of Centres of Excellence, Canada) for financial support.

LA050018T

(37) Leng, J.; Egelhaaf, S. U.; Cates, M. E. *Biophys. J.* **2003**, *85*, 1624−1646.
(38) Brockman, H. *Chem. Phys. Lipids* **1994**, *73*, 57−79.
(39) Katsaras, J.; Donaberger, R. L.; Swainson, I. P.; Tennant, D. C.; Tun, Z.; Vold, R. R.; Prosser, R. S. *Phys. Rev. Lett.* **1997**, *78*, 899−902.
(40) Arnold, A.; Labrot, T.; Oda, R.; Dufourc, E. J. *Biophys. J.* **2002**, *83*, 2667−2680.
(41) Ottiger, M.; Bax, A. *J. Biomol. NMR* **1998**, *12*, 361−372.